17th World Conference on Earthquake Engineering, 17WCEE
Sendai, Japan - September 13th to 18th 2020

NONLINEAR RESPONSE of TONGHAI SOFT SITE in THE AUGUST 2018 TONGHAI EARTHQUAKE, YUNNAN CHINA

J. Cui[(1)], X. Li[(2)], G.Lin[(3)]

[(1)] *Research Fellow, Yunnan Earthquake Agency, hxmcjw@163.com*
[(2)] *Senior Engineer, Yunnan Earthquake Agency, 179298308@qq.com*
[(3)] *Engineer, Yunnan Earthquake Agency, 415942355@qq.com*

Abstract

The two Ms5.0 earthquakes occurred at the edge of Tonghai basin, and were recorded by strong motion stations and downhole array. Tonghai basin is a soft soil faulted lacustrine basin. In order to study the seismic response of soft soil, a three-dimensional downhole array was established near the epicenter of this earthquake about 10 years ago.

The array has 4 observation points on the ground and 4 observation points at different depth. During the earthquake, records of 4 ground points and downhole -60m records were obtained. The epicenter distance of the observation point closest to the epicenter is about 3km. The maximum PGA corresponding to Mw5.0 and Mw4.8 are 0.47g and 0.27g, respectively, and -60m PGA are 0.11g and 0.15g, respectively.

Based on spectral ratio method and DNL index method, we discuss the site earthquake response and results show The site experienced a relatively strong non-linear response.

Keywords: Tonghai Earthquake, Nonlinear Response, Strong Motion records, Downhole Array, DNL Index

1. Introduction

On August 13 and 14, 2018, two earthquakes occurred at 01:44a.m and 03:50a.m Beijing time respectively in the Tonghai region, Yunnan, China with same epicenters at 24.19N, 102.71E, 92km South from the city of Kunming. According to the China Earthquake Network Center(CENC) and the Yunnan Earthquake Monitoring Center (YEMC) , the two earthquake sources are at a shallow depth of 7km and 6km, and had a surface wave magnitude Ms5.0 (http://www.ceic.ac.cn/speedsearch), and but their moment magnitudes are Mw5.0 and Mw4.8 respectively given by Yunnan Earthquake Agency.

The two events are located on the north edge of the Tonghai basin. The Tonghai basin is a fault basin that locates in a tectonically complex and strong earthquake activity region. Its east is the west-branch of NS Xiajiang fault zone that occurred a magnitude 8 earthquake in 1833, the south is the NW-NWW Qujiang fault that occurred Tonghai magnitude 7.8 earthquake near to Tonghai basin, and the west is the NS Puduhe fault. (Wen X. Z, et al. ,2011).

Tonghai basin is a lacustrine soft soil fault basin. In order to study the response of soft soil sites to strong motion, a three-dimensional downhole array was set up on the western edge of the basin in 2008. From 2008, a few records of some events including 2008 Wenchuan Ms8.0 earthquake were obtained by some observation points of the array. In two earthquakes in 2018, the array obtained the free field and downhole records of two mainshocks and some aftershocks at small epicentre distances, and the maximum PGA of the free field is 467gal.

The seismic effects are the important factors of structure damage[1]. While the seismic motion is strong, the seismic effects will present complex non-linear feature, especially in soft soil[2-5]. Based on spectral ratio method, it can be effectively identified whether the site has experienced nonlinear seismic response[6-8]. some researcher have proposed quantitative indexes to measure the degree of the nonlinear site seismic response[8-11]. Based on the obtained observation records , the soil layer model of the site and the spectral ratio method, this paper analyzes the seismic response of the array site. The results show that the array site experienced strong nonlinear response during the two earthquakes.

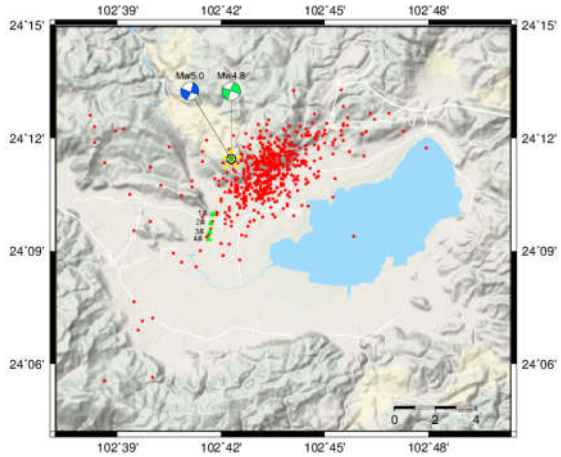

Fig.1 The Array (Green triangle) , the two Earthquakes and their aftershocks(red point)

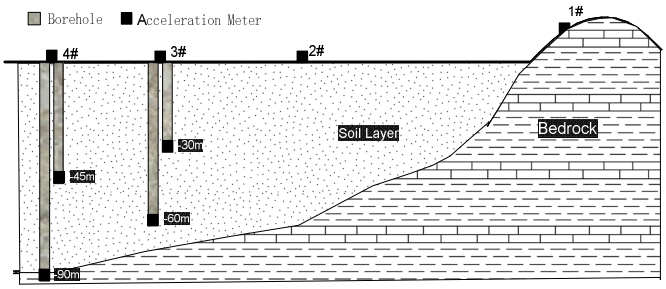

Fig.2 The schematic diagram of the array distribution

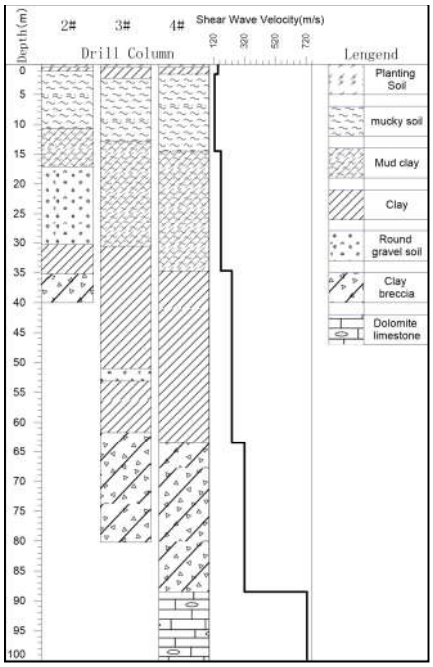

Fig.3 The drill columns in sites of 2#,3# and 4# and the shear wave velocity profile in 4#

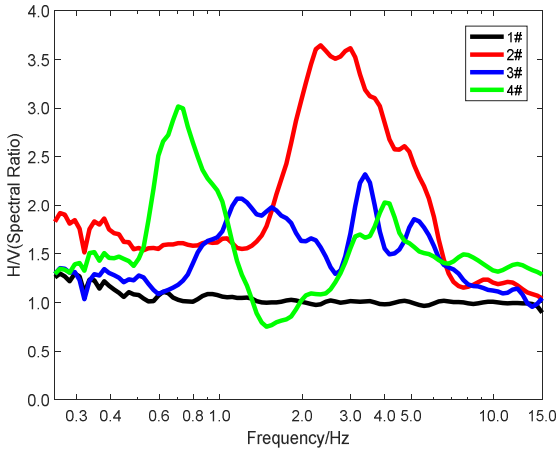

Fig.4 microtremor HVSR curves of the four site

2. The Array and Strong motion records

2.1 Three-dimensional downhole array

The array is deployed on the west of Tonghai fault basin, and constructed with 8 observation point. Fig.1 shows the Tonghai basin, the location of the array and the distribution of the two mainshocks and their aftershocks. Fig.2 shows the schematic diagram of the array three-dimension distribution. In the 8 observation points, the fours are free-filed points, and others are in the downhole in the different depth such as shown in Fig.2. In the 4 free-filed points, 1# site can be regarded as a rock, and the sites of 2#,3# and 4# are all soft soil that their drill columns and Shear wave velocity profile are shown in Fig.3. Fig.4 is microtremor HVSR curves of the four sites, from it, we can see that 1# is nearly to rock site, in general, 4# site is softer than other sites. Depending on Chinese site classification method[12], 1# is type-I site, and 2#,3# and 4# are type-IV site.

2.2 Strong motion records

In the Mw5.0 and Mw4.8 shock, the array obtained respectively 5 records in the 5 observation points that include 4 ground points and one -60m point for some instruments failure, and for 1# closest to the epicenter, only vertical component motion was obtained for other two components failure. Except for two main earthquakes, some aftershocks also were recorded. The Table 1 report the record parameters of two mainshocks and some aftershocks. Fig.5 and Fig.6 are respectively time histories of the two mainshock records.

Table 1. record parameters of two mainshocks

Earthquake	Station Name	Station Code	Epic. Distance/km	Site Class	PGA(gal)	PGV(cm/s)	Arias Intensity
Mw5.0	1#	53SA1	3.0	I	81.4	22.3	5.2
	2#	53SA2	3.4	IV	467.0	45.8	111.3
	3#	53SA3	3.9	IV	429.1	35.7	58.8
	3#(-60m)	53SA5	3.9	IV	106.3	5.6	3.7
	4#	53SA6	4.2	IV	232.7	22.3	34.1
Mw4.8	1#	53SA1	3.0	I	68.6	22.1	3.5
	2#	53SA2	3.4	IV	271.9	23.6	45.1
	3#	53SA3	3.9	IV	262.3	9.2	27.7
	3#(-60m)	53SA5	3.9	IV	114.3	5.7	2.9
	4#	53SA6	4.2	IV	187.7	17.1	18.9
M_L2.6	1#	53SA1	2.2	I	46.4	1.3	0.4
	2#	53SA2	2.8	IV	60.6	2.8	1.6
	3#	53SA3	3.0	IV	56.0	3.0	0.8
	3#(-60m)	53SA5	3.0	IV	17.9	0.6	0.06
	4#	53SA6	3.3	IV	19.5	1.0	0.2
	4#(-45m)	53SA7	3.3	IV	10.5	0.3	0.04
	4#(-90m)	53SA8	3.3	Rock	6.1	0.2	0.006
M_L1.4	1#	53SA1	2.9	I	9.0	0.1	0.01
	2#	53SA2	3.1	IV	7.2	0.2	0.03
	3#	53SA3	3.2	IV	6.9	0.2	0.01
	3#(-60m)	53SA5	3.2	IV	2.2	0.04	0.001
	4#	53SA6	3.4	IV	3.9	0.1	0.002
	4#(-45m)	53SA7	3.4	IV	2.4	0.04	0.0009
	4#(-90m)	53SA8	3.4	Rock	1.1	0.03	0.0001

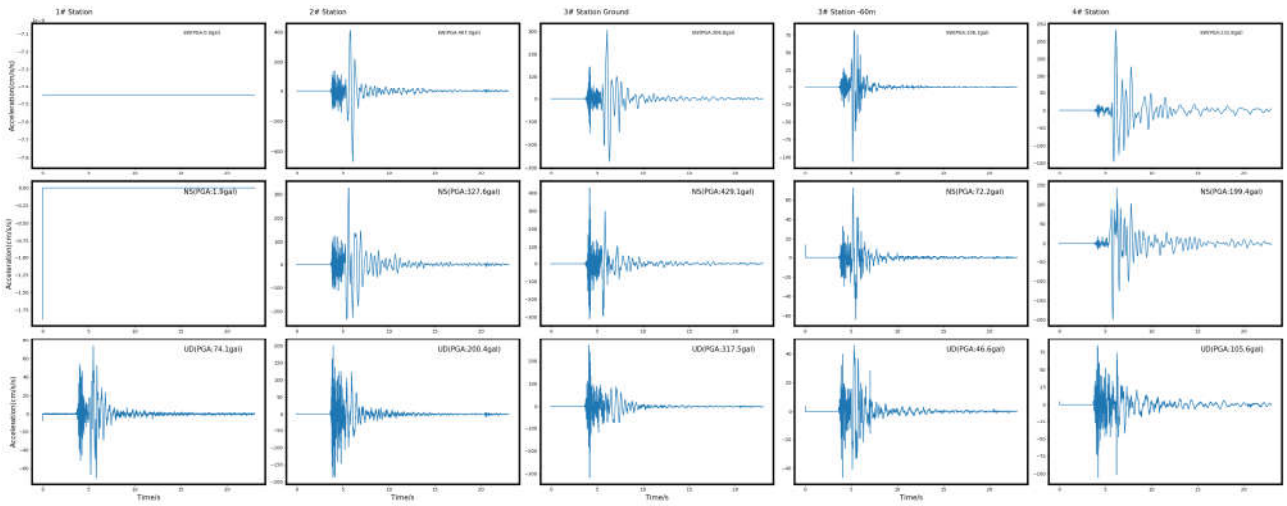

Fig.5 Time Histories of Mw5.0 records

3. Nonlinear Response Analysis of Array Sites

After the seismic response of the site is in a non-linear stage, one of its significant features is that the dominant frequency will reduce and the effect of site amplification will also be weakened[3,7,8]. These two characteristics can be easily and clearly identified by comparing the spectrum ratio of weak and strong earthquake records on the same site. In the case of only ground record, the horizontal-vertical spectral ratio

(HVSR) method is used. The HVSR method is more accurate for judging dominant frequency change, but its reliability is not high in judging the degree of amplitude amplification. For the case of downhole arrays, based on the ground and downhole records, the borehole spectral ratio method(BSR) can get reliable results in both resonance frequency and amplitude amplification. In this section, HVSR and BSR are used to identify the non-linear response at various observation points of the array.

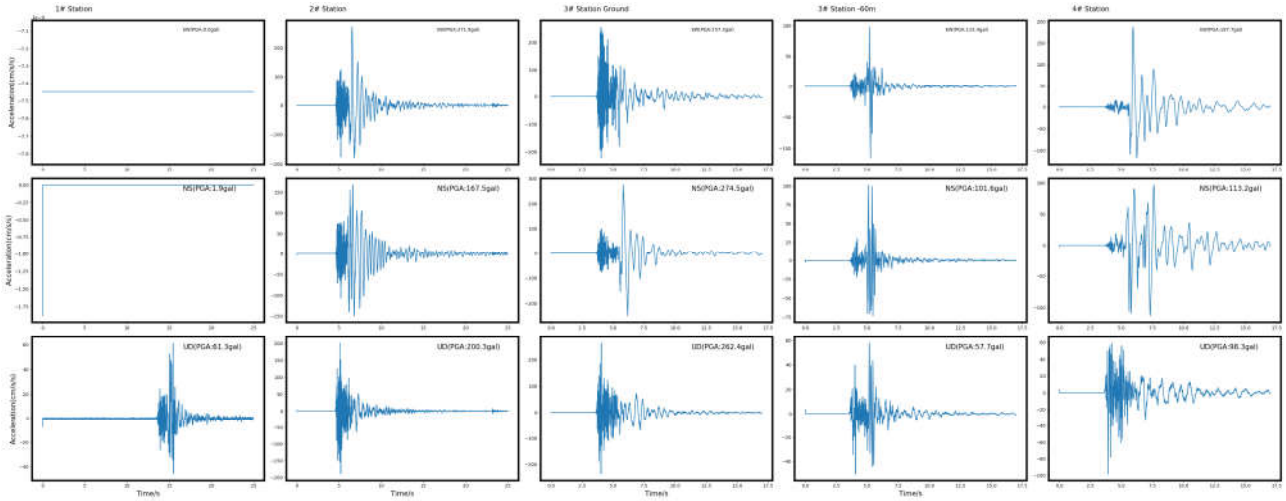

Fig.6 Time Histories of Mw4.8 records

3.1 Horizontal-vertical Spectral Ratio Analysis

For a three component record, its horizontal-vertical Fourier amplitude ratios can be expressed as

$$HVSR(f) = \frac{\sqrt{EW^2 + NS^2}}{UD} \quad \textbf{(1)}$$

where NS, EW and UD are the Fourier amplitude spectra of acceleration record in the NS-, EW- and UD-component, respectively. Eq(1) combines both horizontal effects. While Spectral ratios are calculated, the spectrum is smoothed using Konno-Ohmachi smoothing function[13].

Fig.7-Fig.10 shows HVSR curves of the records on 4 sites, and in Fig.8-Fig.10, the transfer function(TF) from Vs profiles with PySeismoSoil[14] also are showed. In addition to plotting each record HVSR curve, the average of these curves, according to PGA of the records, the HVSR curve is averaged on PGA section.Table 2 shows the amount of records for each PGA section. Due to the lack of NS and EW component records, 1# HVSR curves do not include two main shock records. Except for the 1#, there are only two records for Mw5 and Mw4.8 that thier PGAs are in the two largest PGA sections, so the average HVSR curve of this two sections coincides with the two record HVSR curves.

From Fig.7-10 and Table 2, we can see that with PGA increases, dominant frequencies of HVSR curves become lower on the whole , but HVSR amplitudes do not become small that is not coincide with previous results[3,7,8] , the reason may be that the records in this article are all got in very close to the epicenter that is not suitable completely for the basic assumptions of HVSR. HVSR does not fully reflect the characteristics of the site, and is strongly disturbed by the source. On the other hand, comparing with TF and 3 figures, we can observably find the dominant frequencies of HVSR Curves is low, and the amplitudes are larger.

Table 2 The amount of records for each site PGA section and

PGA	400<PGA	300<PGA<400	200<PGA<300	100<PGA<200	50<PGA<100	PGA<50	Total
1#	0	0	0	0	1/1.11	15/1.78	16/1.78
2#	1/0.60	1/1.09	0/~	2/1.32	2/1.57	22/1.33	28/1.33
3#	1/0.43	1/0.60	0/~	2/0.69	3/0.63	34/0.75	41/0.75
4#	0	1/0.48	1/0.52	0	2/0.57	17/0.56	20/0.56

Note: in table, after "/" is dominant frequency of the mean HVSR curve

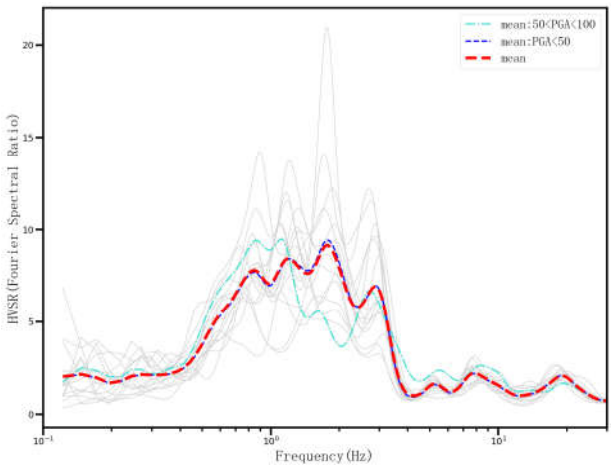

Fig.7 HVSR for 1#

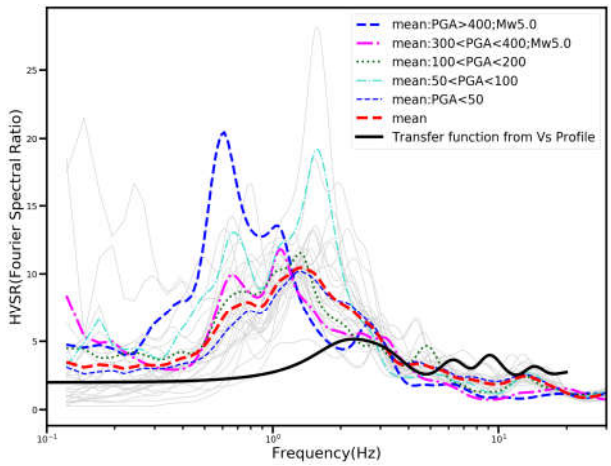

Fig.8 HVSR for 2#

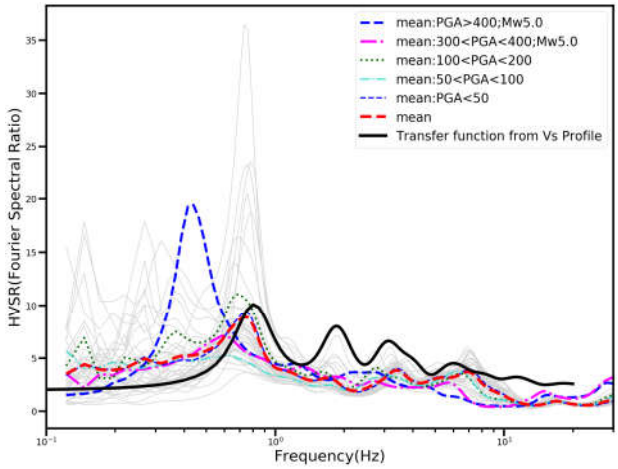

Fig.9 HVSR for 3#

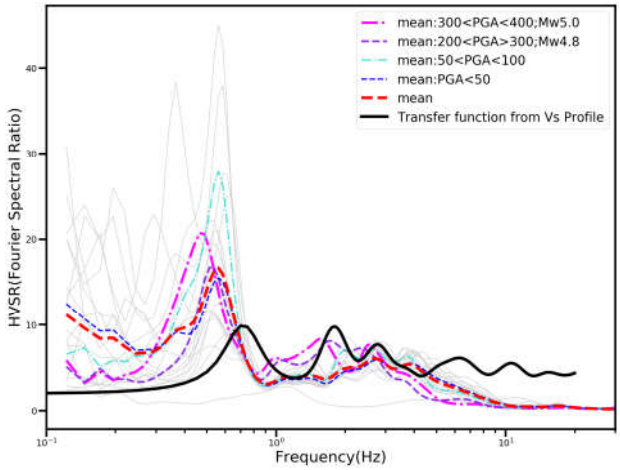

Fig.10 HVSR for 4#

3.2 **Surface-Depth Spectral Ratio Analysis**

The borehole Fourier spectral ratio (BSR) between the surface and downhole records as defined in Eq (2)

$$BSR(f) = \sqrt{\frac{EW_{surf} + NS_{surf}}{EW_{depth} + NS_{depth}}} \qquad \textbf{(2)}$$

in which EW_{surf}, NS_{surf}, EW_{depth}, and NS_{depth} are the Fourier spectra of the east–west and north–south components of the surface and downhole records respectively and the spectrum is smoothed using Konno-Ohmachi smoothing function[13].

Fig.11-Fig.12 shows BSR curves of the records and TFs from Vs profile on 3# and 4#[14]. For BSR, it is same with HVSR that with the PGA increasing, the dominant frequencies of BSR will decrease[15,16]. From Fig.11, we can see the the dominant frequencies of two mainshock BSRs are far less than other small earthquakes. But for the amplitude, they do not show same phenomenon, corresponding to respective dominant frequencies, the BSRs of the two mainshocks are almost the largest in the amplitude. For Fig.12, in terms of mean BSRs, although with the PGA increasing, the dominant frequency offset not obvious, the amplitude decreases significantly. For TF, the dominant frequency of 3# is smaller than other BSR curves, but for 4#, they are nearly same, and for the two sites, the amplitude of TFs is almost smaller than BSRs.

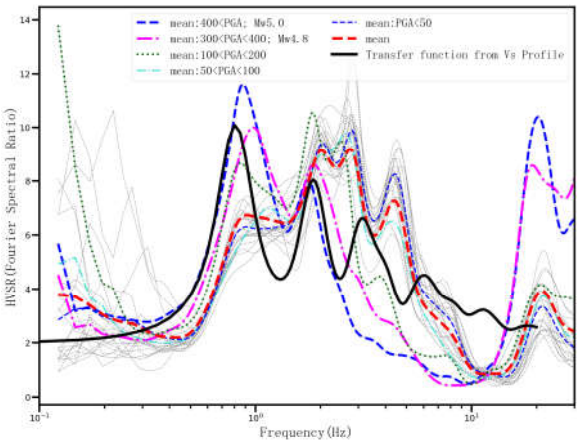

Fig.11 BSR for 3#

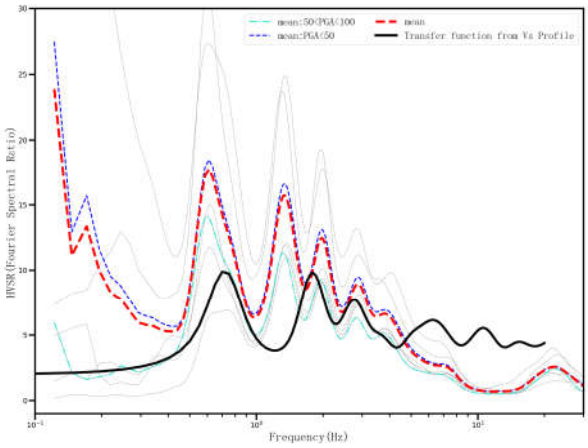

Fig.12 BSR for 4#

3.3 The Quantitative Analysis of Nonlinear Response

Although nonlinear ground responses can be identified with HVSR or BSR, it is a problem that how to quantitatively estimate the degree of nonlinearity of the response. Noguchi and Sasatani defined the following index DNL to evaluate a nonlinear site response[10].

$$DNL = \sum \left| log \left(\frac{R_{Target}(f)}{R_{Reference}(f)} \right) \right| \Delta f \qquad (3)$$

In this equation, the R_{Target} is Surface/Borehole or S-H/V spectral ratio for strong motion data. The $R_{Reference}$ is the reference spectral ratio which is made from weak motion records. Δf is frequency interval.in this paper, *DNL* is computed within the frequency range 0.2-20.

Fig.13 and Fig.16 show the DNL computation of Mw5.0 earthquake from HVSR and BSR that represent with the subscripts hvsr and BSR, respectively. In the calculation, the two Reference is selected: one is a small earthquake record that can maximize the DNL value of the two main shock records; secondly, the average value of HVSRs or BSRs of recordings that PGAs are smaller than 50gal. The areas between the Target and the two References are simultaneously represented in the four figures in yellow and green, when the two areas overlap, the color is changed to yellow green. Table 3 is the DNL values of two mainshocks on four sites.

According to Noguchi et al.[17], when the nonlinear response occurs, DNL> 4.0. Depending on this threshold value, in two large earthquakes, the response of the 3 sites in table 3 is non-linear. It can be seen that the DNL calculated from the BSR is greater than the result obtained from the HVSR, and the DNL from the average value Reference is smaller. That means that DNL is a relative value that depends on which the Reference is adopted. Fig.17 is the relationship between DNL_{hvsr} and PGA. It can be seen that when PGA is small, the DNL value is very discrete, but after PGA>100 gal, the discrete decrease and DNL increases with the increase of PGA. Due to dependency on Reference and the discrete while PGA is small, DNL is not good index for identifying the non-linear response of a site. Its application should be in conjunction with PGA.

Although the PGAs in 2# are larger than in other two sites, its DNL in the table is smaller than or equal to other two. Given that the other two sites are softer, this result should be reasonable. Comparing 2#, non-linear responses are more intense at the other two sites.

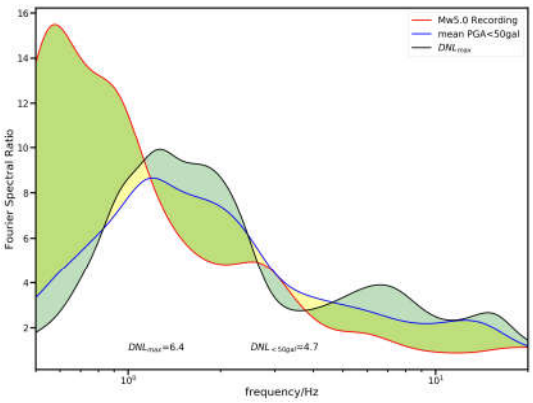

Fig.13 2# DNL_{hvsr} of Mw5.0 record

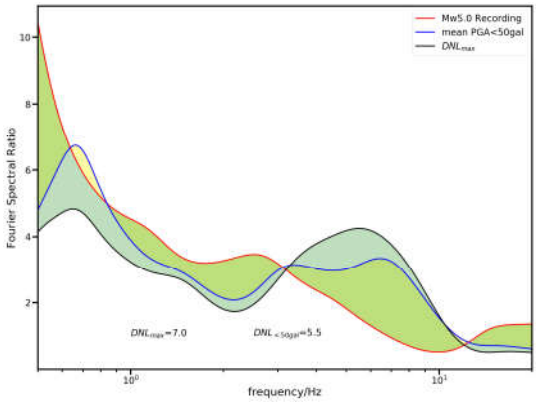

Fig.14 3# DNL_{hvsr} of Mw5.0 record

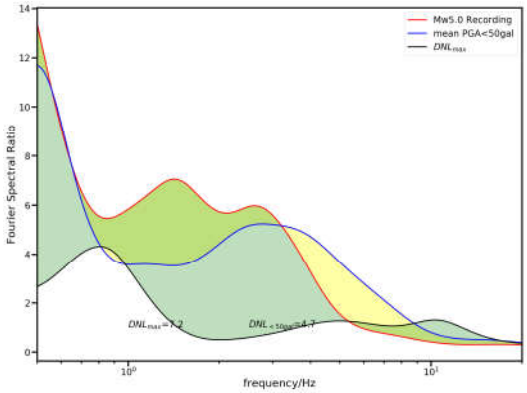

Fig.15 4# DNL_{hvsr} of Mw5.0 record

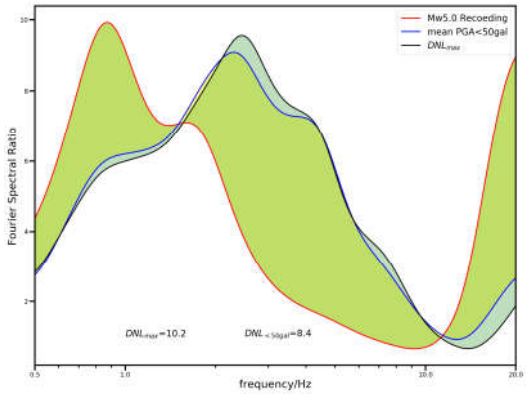

Fig.16 3# DNL_{BSR} of Mw5.0 record

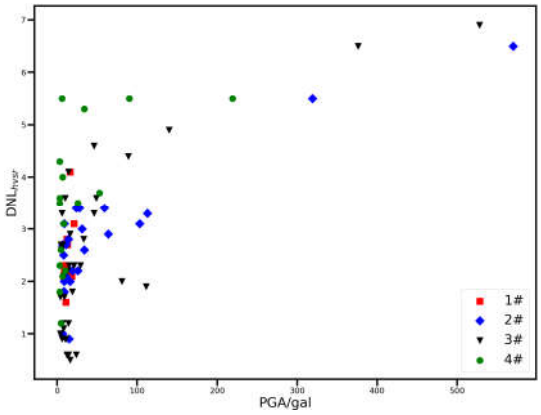

Fig.17 the relation of DNL_{hvsr} *with PGA in four site*

Table 3 the DNL values of two mainshocks on four sites

Site	Mw5.0		Mw4.8	
	DNL_{hvsr}	DNL_{BSR}	DNL_{hvsr}	DNL_{BSR}
2#	6.4		5.4	
3#	7.0	10.2	6.3	9.7
4#	7.2		5.4	

4. Conclusions

Using HVSR, BSR and DNL methods, this paper investigated the nonlinear soil response characteristics at Tonghai soft site in two mainshocks based the records of Tonghai array. The results show that the nonlinear site effects existed in Tonghai soft site. Although the PGAs in 2# are

largest, its DNL is smallest, and non-linear responses are more intense at 3# and 4#. Many researchers have pointed out that the reduction of dominant frequency and amplitude are two nonlinear identification indexes of HVSR and BSR, but we only find the reduction of dominant frequency, the reasons are needed to be further studied.

DNL is a convenient quantitative index to identify the nonlinear response. However, DNL is heavily dependent on the Reference, and its discrete is large when the PGA is smaller than 100gal. As a separate index, its reliability is not high and should be combined with PGA to identify non-linear site response.

5. Acknowledgements

This work is supported by the National Natural Science Foundation of China (Grant No.*51578514*)

6. Copyrights

References

[1] Beresnev, IA., and Wen K. (1996): Nonlinear soil response—A reality? Bulletin of the Seismological Society of America, 86:1964–1978.

[2] Field EH, Johnson PA, Beresnev IA, Zeng Y(1997): Nonlinear ground motion amplification by sediments during the Northridge earthquake. Nature, 390:599–602.

[3] Beresnev IA, Atkinson GM, Johnson PA, Field EH (1998): Stochastic finite fault modeling of ground motions from the Northridge California, earthquake. II. Widespread nonlinear response at soil sites. Bulletin of the Seismological Society of America, 88:1402–1410.

[4] Yu G, Anderson JG, Siddharthan R (1992): On the characteristics of nonlinear soil response. Bulletin of the Seismological Society of America, 83:218–244.

[5] Beresnev IA (2002): Nonlinearity at California Generic Soil Sites from Modeling Recent Strong-Motion Data. Bulletin of the Seismological Society of America, 92(2):863–870..

[6] Wen, K. L., Chang, T. M., Lin, C. M. and Chiang, H. J (2006). Identification of Nonlinear Site Response Using the H/V Spectral Ratio Method. Terr. Atmos. Ocean. Sci., 17(3):533-546.

[7] Dimitriu P., I.Kalogeras, N.Theodulidis(1999). Evidence of nonlinear site response in horizontal-to-vertical spectral ratio from near-field earthquakes. Soil Dynamics and Earthquake Engineering, 18(6):423-435.

[8] Noguchi, S. and Sasatani, T. (2008): Quantification of degree of nonlinear site response. 14th World Conference on Earthquake Engineering, 03-03-0049.

[9] Noguchi, S., Sato H., Sasatani, T. (2012): Characterization of Nonlinear Site Response Based on Strong Motion Records at K-NET and KiK-net Stations in the East of Japan. 15th World Conference on Earthquake Engineering, 03-03-0049.

[10] Regnier J, Cadet H, Bonilla L F, et al (2013). Assessing nonlinear behavior of soils in seismic site response: statistical analysis on KiK-net strong-motion data [J]. Bulletin of the Seismological Society of America, 103(3): 1750–1770.

[11] Régnier J., Cadet H, Bard PY (2016). Empirical Quantification of the Impact of Nonlinear Soil Behavior on Site Response. Bulletin of the Seismological Society of America, 106 (4): 1710–1719.

[12] Code for seismic design of buildings: GB 50011—2010[S]. Beijing: China Architecture & Building Press，2010．(in Chinese)

[13] Katsuaki Konno, Tatsuo Ohmachi (1998) Ground-motion characteristics estimated from spectral ratio between horizontal and vertical components of microtremor. Bulletin of the Seismological Society of America, 88 (1): 228–241.

[14] Asimaki, D., Shi J. (2017). PySeismoSoil Documentation. https://pyseismosoil.readthedocs.io/en/latest/index.html.

[15] Régnier, J., Cadet, H., and Bard, P.-Y. (2017). "Impact of non-linear soil behavior on site response amplitude." 16th World Conference on Earthquake Engineering, Santiago, Chile.

[16] Castro Cruz, David & Bertrand, Etienne & Régnier, Julie & Courboulex, Françoise. (2017). Seismic Non-Linear Behavoir of Soil Inferred by the Analysis of the Kik-Net Borehole Data. 16th European conference on Earthquake Engineering(http://papers.16ecee.org/files/DT%206%20pdf.pdf).

[17] Noguchi S, Sasatani T. Nonlinear Soil Response and Its Effects on Strong Ground Motions during the 2003 Miyagi-Oki Intraslab Earthquake [J]. Zisin, 2012,63(4):255-256.

